Received: 18 June 2025 | Accepted: 28 September 2025

DOI: 10.1002/csc2.70188

Crop Science

ORIGINAL ARTICLE

Genomics, Molecular Genetics & Biotechnology

Comprehensive characterization of HMA transporters in common bean: Tissue-specific expression and response to metal stress

Wenderson Felipe Costa Rodrigues[1] | **Laura Oliveira Pires**[1] | **Lucas Roberto Oliveira**[2] | **Juliane K. Ishida**[1,2,3]

[1]Department of Botany, Institute of Biological Sciences (ICB), Federal University of Minas Gerais (UFMG), Belo Horizonte, Brazil

[2]Center for Nuclear Energy in Agriculture (CENA), University of São Paulo (USP), Piracicaba, Brazil

[3]Department of Genetics, Luiz de Queiroz College of Agriculture (ESALQ), University of São Paulo (USP), Piracicaba, São Paulo, Brazil

Correspondence
Juliane K. Ishida, Department of Genetics, Luiz de Queiroz College of Agriculture (ESALQ), University of São Paulo (USP), Avenida Pádua Dias, 11, Piracicaba, SP, Brazil.
Email: julianeishida@usp.br

Assigned to Associate Editor Alvaro Sanz-Saez.

Funding information
Fundação de Amparo à Pesquisa do Estado de Minas Gerais, Grant/Award Number: APQ-02786-21; Coordenação de Aperfeiçoamento de Pessoal de Nível Superior, Grant/Award Number: Finance Code 001; Instituto Serrapilheira, Grant/Award Number: R-2111-40087; Science Without Borders Program from the Brazilian Federal Government

Abstract

Plant growth and development require tightly regulated concentration of heavy metal ions, which function as essential nutrients. In this context, the P1B-heavy metal ATPase (HMA), also known as the HMA family, is critical for mediating metal ion uptake, root-to-shoot translocation, and vacuolar sequestration in plants. This study presents a comprehensive characterization of 11 HMA genes in *Phaseolus vulgaris* L. (*PvHMA*). Phylogenetic analysis classified the *PvHMAs* genes into six distinct clusters, supported by conserved gene structure and motif distributions. *PvHMA1*, *-2*, *-5*, *-6*, *-7*, and *-11* exhibited widespread expression across multiple tissues and harbored a diverse array of cis-regulatory elements in their promoter, suggesting multiple roles in plant growth and development. In contrast, *PvHMA3* and *PvHMA8* displayed tissue-specific expression patterns, being predominantly expressed in roots and leaves, respectively. Under zinc stress, *PvHMA1*, localized in chloroplasts, showed marked upregulation in shoot tissue. Notably, this transcriptional response was not observed under copper exposure, despite the high structural similarity between PvHMA1 and its *Arabidopsis thaliana* homolog, AtHMA1 (where AtHMA is *Arabidopsis thaliana* HMA). *PvHMA2*, an ortholog of the *A. thaliana* HMA2/4, exhibited increased sensitivity to cobalt stress. Additionally, *PvHMA5* and *-11* were differentially expressed in shoots in response to zinc treatment. Collectively, these findings provide a detailed overview of the HMA family in *P. vulgaris* and reveal a complex regulatory network of transporters involved in heavy metal homeostasis, with implications for plant nutrition, development, and stress responses.

Abbreviations: AtHMA, *Arabidopsis thaliana* HMA; HM, heavy metal; HMA, Heavy Metal ATPase; OsHMA, *Oryza sativa* HMA; PvHMA, *Phaseolus vulgaris* L. HMA; RMSD, Root-mean-square deviation; SOD, superoxide dismutase; TM, transmembrane.

Wenderson Felipe Costa Rodrigues and Laura Oliveira Pires contributed equally to this work.

Plain Language Summary

Plants need certain metal ions, like zinc and copper, to grow properly. Special proteins called heavy metal ATPases (HMAs) help move these metals around the plant and store them safely. In this study, we looked at *HMA* genes in common bean plants (*Phaseolus vulgaris*). We grouped the genes into six families and found that some are active in many plant parts, while others work mainly in roots or leaves. When the plants were exposed to zinc, some genes, like *PvHMA1* (where PvHMA is *Phaseolus vulgaris* L. HMA) and *PvHMA2*, changed their activity, especially in shoots. These changes did not happen under copper stress. Our results show that *HMA* genes help plants manage metal nutrients and respond to stress. This research could help improve plant health and nutrition.

1 | INTRODUCTION

Heavy metals (HMs) are generally defined as transition and post-transition elements with high density (Hawkes, 1997). This broad category includes more than 20 elements, some of which are highly toxic, such as mercury (Hg), arsenic (As), lead (Pb), cadmium (Cd), cobalt (Co), copper (Cu), manganese (Mn), molybdenum (Mo), nickel (Ni), and zinc (Zn). At elevated concentration, these elements interfere with key cellular functions by inactivating metabolic enzymes, disrupting membrane integrity, and inducing excessive production of reactive oxygen species (Rascio & Navari-Izzo, 2011). However, when present at optimal levels, several HMs function as micronutrients contributing to proper plant growth and development (Alloway, 2013). The intensive and prolonged use of chemical fertilizers in crop cultivation has led to a significant accumulation of HMs in the soil (Atafar et al., 2010), resulting in environmental contamination (Mortvedt, 1996), negative impacts on human health (Mortvedt, 1996), and alteration in the structure and function of soil microbial communities (Navarrete et al., 2017). Understanding the molecular mechanisms that regulate the uptake, translocation, and sequestration of HMs in plants is critical for defining the thresholds at which these elements transition from being beneficial to toxic.

Among the proteins involved in HM homeostasis, members of the P-type ATPase superfamily play a central role. These transporters utilize ATP hydrolysis to mediate the active transport of cations across biological membranes against their electrochemical gradients (Hanikenne & Baurain, 2014). The "P-type" designations refer to the transient formation of a phosphorylated intermediate during the transport cycle (Pedersen & Carafoli, 1987). P-type ATPases are conserved across all domains of life and participate in a wide range of cellular processes (Farley, 2012). Based on substrate specificity, they are classified into five major subfamilies (P1–P5) (Palmgren & Axelsen, 1998). For instance, the H+ATPase in plants and fungi belongs to the P3A-type, whereas Na^+/K^+ and Ca^{2+}ATPases in animals fall under the P2C/D- and P2A/B-types, respectively (Kühlbrandt, 2004). The P1B-type ATPases, also known as heavy metal ATPase (HMA), form a distinct subgroup specialized in the transport of transition metals. These proteins are characterized by the presence of eight transmembrane (TM) domains, including a highly conserved CPx motif (cysteine-proline-cysteine, cysteine-proline-histidine, or cysteine-proline-serine) within the sixth TM domain, which is responsible for metal ion binding (Hanikenne & Baurain, 2014). Additionally, HMAs possess five conserved signature motifs—DKTGT, GDGxNDxP, PxxK, HP, and S/TGE—that are critical for ATP hydrolysis and metal transport (Argüello et al., 2007). Understanding the function and regulation of HMA transporters is essential for advancing strategies in phytoremediation, crop biofortification, and tolerance to metal stress.

Plant HM transporters play a crucial role in the tolerance of HMs and in maintaining the balance of metal ions inside the plant (Williams et al., 2000). The HMA family of transporters can be categorized into two subgroups: one that binds to monovalent ions such as Cu^+ and Ag^+, and another that is linked with divalent ions including Zn^{2+}, Cd^{2+}, Pb^{2+}, and Co^{2+} (Axelsen & Palmgren, 2001). The *Arabidopsis thaliana* genome contains eight members (Baxter et al., 2003). Among them, *AtHMA2* (where *AtHMA* is *Arabidopsis thaliana* HMA)and *AtHMA4* are expressed in vascular tissues and produce proteins involved in metal translocation through the xylem (Hussain et al., 2004; Sinclair et al., 2007). In the related species *Arabidopsis halleri*, constitutive expression of *HMA4* is directly associated with the species' ability to tolerate and hyperaccumulate Zn and Cd (Nouet et al., 2015). Enhanced metal tolerance in *A. thaliana* can be achieved by overexpressing *AtHMA3*, a tonoplast-localized transporter that facilitates vacuolar sequestration of toxic metals (Morel et al., 2009). Transgenic lines overexpressing *AtHMA3* exhibit enhanced tolerance to Cd, Zn, Pb, and Co, while mutants

lacking this transporter show increased sensitivity, particularly to Cd and Zn stress (Morel et al., 2009). Similar findings have been reported in other species; for example, transgenic tobacco expressing *SaHMA3h* from *Sedum alfredii* displayed improved cadmium tolerance and accumulation (Z. Zhang et al., 2016). In *Brassica rapa*, variations in leaf cadmium content were linked to differential expression of *BjHMA3* (L. Zhang et al., 2019). Additionally, ectopic expression of *OsHMA3* (where *OsHMA* is *Oryza sativa* HMA) in rice resulted in greater Cd tolerance and reduced Cd levels in aerial tissues and grains, while increasing Cd accumulation in the roots (Ueno et al., 2010). The AtHMA1, localized in the chloroplast envelope, is known for its role in copper translocation (Seigneurin-Berny et al., 2006). This transporter is essential for delivering Cu to superoxide dismutase (SOD), a key enzyme that mitigates oxidative stress generated during photosynthesis (Seigneurin-Berny et al., 2006). Under Zn (II) excess, AtHMA1 also contributes to detoxification by removing Zn from plastids (Kim et al., 2009). In addition to Cu, AtHMA1 has been shown to interact with calcium, functioning in association with calcium ATPase (Moreno et al., 2008). AtHMA5–8 are predicted to mediate the transporter of Cu and silver (Ag). AtHMA6 (AtPAA1) and AtHMA8 (AtPAA2) are both involved in chloroplast Cu homeostasis. AtHMA6 is located in the plastid envelope, while AtHMA8 is situated in the thylakoid membranes (Abdel-Ghany et al., 2005; Shikanai et al., 2003). AtHMA5 is primarily involved in Cu detoxification in roots (Andrés-Colás et al., 2006). Lastly, AtHMA7, also known as RAN1, delivers Cu to post-Golgi compartments and is essential for maturation of ethylene receptors (Hirayama et al., 1999). The *Oryza sativa* (rice) genome encodes nine HMA genes, with OsHMA1–3 belonging to the Zn/Co/Cd/Pb group and OsHMA4–9 belonging to the Cu/Ag group (Baxter et al., 2003). Among these, OsHMA2 plays a key role in the translocation of Zn/Cd from root cells to vascular tissues, thereby promoting their movement from roots to shoots (Satoh-Nagasawa et al., 2012; Takahashi et al., 2012). OsHMA3 transports and stores Cd ions in vacuoles within root cells, while OsHMA9 facilitates the export of Cu and Zn ions from the cells to the apoplastic region (Lee et al., 2007).

Phaseolus vulgaris L., commonly known as the common bean, represents the most significant grain legume for direct human consumption globally (Food and Agriculture Organization [FAO], www.fao.org/faostat). Cultivated extensively, it constitutes a staple food for millions of individuals, particularly in Latin America and Africa, where it serves as a primary source of dietary sustenance (FAO, www.fao.org/faostat). The crop's importance is multifaceted, encompassing both nutritional and agronomic dimensions. Nutritionally, common beans provide a cost-effective source of high-quality protein, complex carbohydrates, dietary fiber, and essential micronutrients, notably iron (Fe) and zinc (Murube et al., 2021), and thus play a critical role in public health strategies addressing malnutrition. Its widespread consumption and nutrient density render it a suitable candidate for biofortification programs (Sperotto & Ricachenevsky, 2017) aimed at mitigating hidden hunger, particularly micronutrient deficiencies such as iron deficiency anemia, which affects billions worldwide. From an agricultural perspective, common beans contribute to sustainable farming systems through symbiotic associations with nitrogen-fixing *Rhizobia*, enhancing soil fertility and reducing reliance on synthetic fertilizers (Abd-Alla et al., 2023). Understanding the molecular components involved in HM homeostasis in *P. vulgaris* is fundamental to improving our knowledge of how micronutrients are taken up from the soil and allocated to edible plant tissues. This insight has the potential to inform strategies aimed at enhancing nutritional content and developing biofortified cultivars. Although members of the HMA gene family have been identified and characterized in several plant species, including *Glycine max* (soybean) (Fang et al., 2016), *Populus trichocarpa* (D. Li et al., 2015), *Brassica napus* (N. Li et al., 2018), maize, *Triticum aestivum* (Batool et al., 2023), *Medicago truncatula* (Ma et al., 2021), and sorghum (Zhiguo et al., 2018), a systematic and comprehensive analysis of these genes in common beans is still lacking. In this study, we performed a genome-wide analysis of 11 putative *HMA* homologs in *P. vulgaris* L. (*PvHMA*). We examined their gene structure, phylogenetic relationships, conserved motifs, and cis-regulatory elements. Furthermore, we analyzed publicly available gene expression datasets to evaluate the transcriptional profiles of P*vHMA* genes during different developmental stages and under metal stress conditions. Structural modeling was also employed to explore the three-dimensional (3D) conformation of selected PvHMA proteins. Together, these findings provide a foundational framework for future functional studies on HMA transporters in common beans, with implications for improving nutrient use efficiency, stress resilience, and biofortification strategies.

2 | MATERIALS AND METHODS

2.1 | Plant material and growth conditions

Seeds of *P. vulgaris* cultivar Carioca IAC-Alvorada were germinated in a climate-controlled growth chamber at 25˚C–28˚C with a 12-h light/12-h dark photoperiod. Plants were grown in saturated vermiculate for 14 days. Following this period, the substrate was carefully removed, and the roots were washed thoroughly. To assess the effects of HM stress, roots were immersed in aqueous solutions containing divalent metal salts at the following concentrations: 50 μM cobalt chloride ($CoCl_2$), 100 μM copper sulfate ($CuSO_4$), 150 μM nickel chloride ($NiCl_2$), or 200 μM zinc sulfate ($ZnSO_4$). Control plants were treated with demineralized water under the same

conditions. Treatments were applied for two exposure periods, 2 and 18 h, to simulate both short- and long-term stress conditions. Following exposure, roots and shoots tissues from at least two plants per treatment were harvested separately and immediately flash-frozen in liquid nitrogen. All samples were stored at −80°C until further processing. Three independent biological replicates were performed for each treatment condition.

2.2 | Identification and phylogenetic tree construction of HMAs

The AtHMAs protein sequences were retrieved from the *A. thaliana* genome (TAIR10) (Supporting Information S1) via the Phytozome database (http://www.phytozome.net/) and subsequently used as queries in BLASTP (Protein-Protein Basic Local Alignment Search Tool) searches against the *P. vulgaris* genome (G19833) proteome, also accessed through the Phytozome platform. PvHMA homologs were identified based on a minimum similarity threshold of 50%. For each identified gene, the corresponding genomic DNA, coding DNA sequence (CDS), and protein sequences were retrieved. Additional parameters such as protein length, molecular weight (mw), and isoelectric point (pI) were calculated using the Compute pI/Mw (Bjellqvist et al., 1993). Subcellular localization predictions were performed using the TargetP1.1 Server (Emanuelsson et al., 2007) with default parameters. Gene structure was performed using the online tool GSDS 2.0 (http://gsds.cbi.pku.edu.cn) (Hu et al., 2015). Conserved motifs among PvHMA proteins were identified using the MEME Suite (Bailey et al., 2009), under default settings. To investigate evolutionary relationships, full-length HMA protein sequences from *P. vulgaris*, *A. thaliana*, *O. sativa* (Baxter et al., 2003), and *G. max* (Fang et al., 2016) were aligned using the CLUSTALW algorithm (Thompson et al., 2002). Phylogenetic trees were constructed with MEGA7 software (Kumar et al., 2016) using the maximum likelihood method with 10,000 bootstrap replications. Hierarchical clustering of PvHMA protein sequences was performed using the GenePattern 2.0 platform (Reich et al., 2006). Pearson correlation coefficients (absolute value) were used as the similarity metric, and the pairwise average-linkage method was applied for clustering. Protein domain comparisons were performed using the SMART database version 7.0 (Letunic et al., 2021), and sequence relationships were constructed with MAFFT (Katoh & Standley, 2013).

2.3 | Promoter region analysis and gene expression profiling

The whole-genome sequence of *P. vulgaris* was obtained from the Phytozome database (https://phytozome.jgi.doe.gov). Putative promoter regions, defined as 1 kb upstream of the translation start site (ATG), were extracted for each PvHMA gene using the GENEIOUS software (www.geneious.com). Cis-regulatory elements within these promoter sequences were identified by PlantCARE (Lescot et al., 2002). Organ-specific expression data for the *PvHMA* genes were retrieved from the Phytozome platform, accessed through user login credentials registered in the JG1 genome portal. The *P. vulgaris* transcriptome dataset (P. vulgaris_442_ver2.1) was downloaded for transcript-level analysis. All graphical elements and figures were created and refined using Adobe Illustrator (Adobe Systems Inc.).

2.4 | RNA isolation and quantitative real-time PCR (RT-qPCR)

Total RNA was extracted from root and shoot tissues using the TRIzol reagent (ThermoFisher Scientific, cat. No. 15596026), following the manufacturer's instructions. To remove residual genomic DNA contamination, RNA samples were treated with DNase I Amplification Grade (ThermoFisher Scientific, cat. No. 1806015). First-strand cDNA synthesis was performed using the High-Capacity cDNA Reverse Transcription Kit (Applied Biosystems, Code 4368814), according to the manufacturer's instructions. The qRT-PCR was carried out using the SyBR Green PCR Master Mix (Applied Biosystems, Code 439155) on a real-time PCR detection system. Relative gene expression levels were calculated using the standard curve method. Primer sequences used in the study are listed in Supporting Information S2. As detailed in the figure legends, gene expression quantification was based on three independent biological replicates, except for Shoot 2 h and Root 18 h samples treated with Zn and Co for *PvHMA6*, where only two biological replicates were used due to limited plant material. Each biological replicate consisted of pooled tissues from at least two individual plants and was analyzed with three technical replicates. To determine statistical significance among treatments, p-values were calculated using the Student's t-test (two-sample assuming equal variances) in Microsoft Excel. Differences were considered significant at $p < 0.05$ and marginally significant at $p < 0.1$.

2.5 | Protein three-dimensional structure prediction of PvHMA

Prior to 3D structure modeling, signal peptides were predicted in SignalP v6.0 (Teufel et al., 2022) and, if identified, removed from the original sequence. However, no PvHMA showed signal peptide via SignalP. Three-dimensional struc-

ture modeling was done via ColabFold (Mirdita et al., 2022), which easily enables structure prediction using AlphaFold2 software (Jumper et al., 2021). Predicted structures were relaxed using Amber force fields and complex prediction (Eastman et al., 2017), where five models were generated, and the highest ranked conformation was selected based on its Predicted Local Distance Difference Test (pLDDT) confidence score. We used PyMOL (pymol.org) to visualize the structures and to know the root-mean-square deviation (RMSD) value of alpha carbon (Cα) atomic positions with the alignment plugin. The TM topology was predicted using DeepTMHMM (Hallgren et al., 2022) and later identified in the modeled proteins.

3 | RESULTS

3.1 | Identification and classification of HMA genes in the *P. vulgaris* genome

To identify members of the HMA gene family in *P. vulgaris*, BLASTP searches were performed against the common bean genome using the *A. thaliana* HMA protein sequence as queries via the Phytozome database. A total of 11 putative *PvHMA* genes were identified. Conserved motif organization and phylogenetic relationships among the predicted proteins were visualized simultaneously (Figure 1A). Key conserved motifs characteristic of the HMA family, including DKTGT, GDGxNDxP, PxxK, S/TGE, HP, and CPx/SPC, were identified across the sequences (Figure 1B), consistent with previously reported HMA features (Argüello et al., 2007). PvHMA sequences contain structural features similar to those found in their homologs in *A. thaliana*, which include the ATPase and hydrolase protein families. A detailed analysis revealed the presence of several conserved domains: the HMA domain (PF00403), the E1-E2 ATPase domain (PF00122), and the hydrolase domain (PF00702) (Supporting Information S3).

Phylogenetic clustering revealed subgroups with distinct motif profiles. Specifically, PvHMA2/3, PvHMA6/8, PvHMA4/7, and PvHMA5/9/10 each shared a set of conserved motifs within their respective clades, whereas PvHMA1 and PvHMA11 exhibited divergent motif compositions (Figure 1A). To investigate the gene structure of PvHMA family members, intron/exon organization was analyzed by aligning genomic sequences with their corresponding coding sequences (CDS) (Figure 2). This analysis revealed significant variation in intron size and distribution across different phylogenetic branches. Additional structural features were examined, including gene, transcript, and CDS lengths (Supporting Information S4). The PvHMA1 and -6 had longer genomic sequences (16,431 and 24,584 bp, respectively), suggesting the presence of large intronic regions (Supporting Information S4). In contrast, transcript lengths across the family were relatively uniform, ranging from 2865 to 3941 bp (Supporting Information S4), supporting the hypothesis of extensive intronic expansion in these two genes. Predicted protein lengths varied from 826 to 1187 aa, with corresponding molecular weights ranging from 90 to 130.9 kDa, and the p*I* between 5.26 and 8.69 (Supporting Information S4). Subcellular localization was predicted using TargetP 1.1 to infer the potential biological role of each transporter. PvHMA1, -6, and -8 were predicted to localize to the chloroplast, while PvHMA5 and -10 were associated with the mitochondrial membrane (Supporting Information S4). PvHMA2 was predicted to be directed toward the secretory pathway, whereas PvHMA3, -4, -7, -9, and -11 lacked identifiable targeting signals (Supporting Information S4). Taken together, the variation in gene structure, conserved motifs, predicted physicochemical properties, and subcellular localization patterns suggests that PvHMA transporters play diverse roles in metal homeostasis and possibly participate in distinct molecular and physiological processes within the common beans.

3.2 | Structural modeling reveals potential biological functions of PvHMA proteins

To gain further insight into the structural and functional differentiation of PvHMA proteins, we selected PvHMA1 and PvHMA5 for comparative 3D modeling, as they were predicted to localize to different subcellular compartments (chloroplast and mitochondrion, respectively). Despite PvHMA5 having a longer amino acid sequence, both proteins shared similar topologies as predicted by DeepTMHMM, featuring eight TM domains and substantial orientation within the interior of their respective organelles (Figure 3A; Supporting Information S5). Protein structure prediction using AlphaFold2 (via the ColabFold platform) generated high-confidence 3D models for both proteins, revealing the organization of TM helices, conserved domains, and relative orientations of intra- and extra-organellar regions (Figure 3B; Supporting Information S6). Both PvHMA1 and PvHMA5 contained the conserved CPx motif within TM6, a signature of HMA transporters. However, in PvHMA1, the canonical cysteine residue was replaced by serine—an alteration also observed in its *A. thaliana* homolog, AtHMA1 (Figure 3C). Structural superposition of PvHMA1 and AtHMA1 revealed a high degree of similarity, with an RMSD of 0.69 Å (Figure 3D; see also Figure 1A). In contrast, structural alignment between PvHMA1 and PvHMA5 resulted in a higher RMSD value of 1.91 Å (Figure 3E), indicating substantial divergence despite shared membrane topology. This structural differentiation may reflect distinct metal specificity or transport mechanisms.

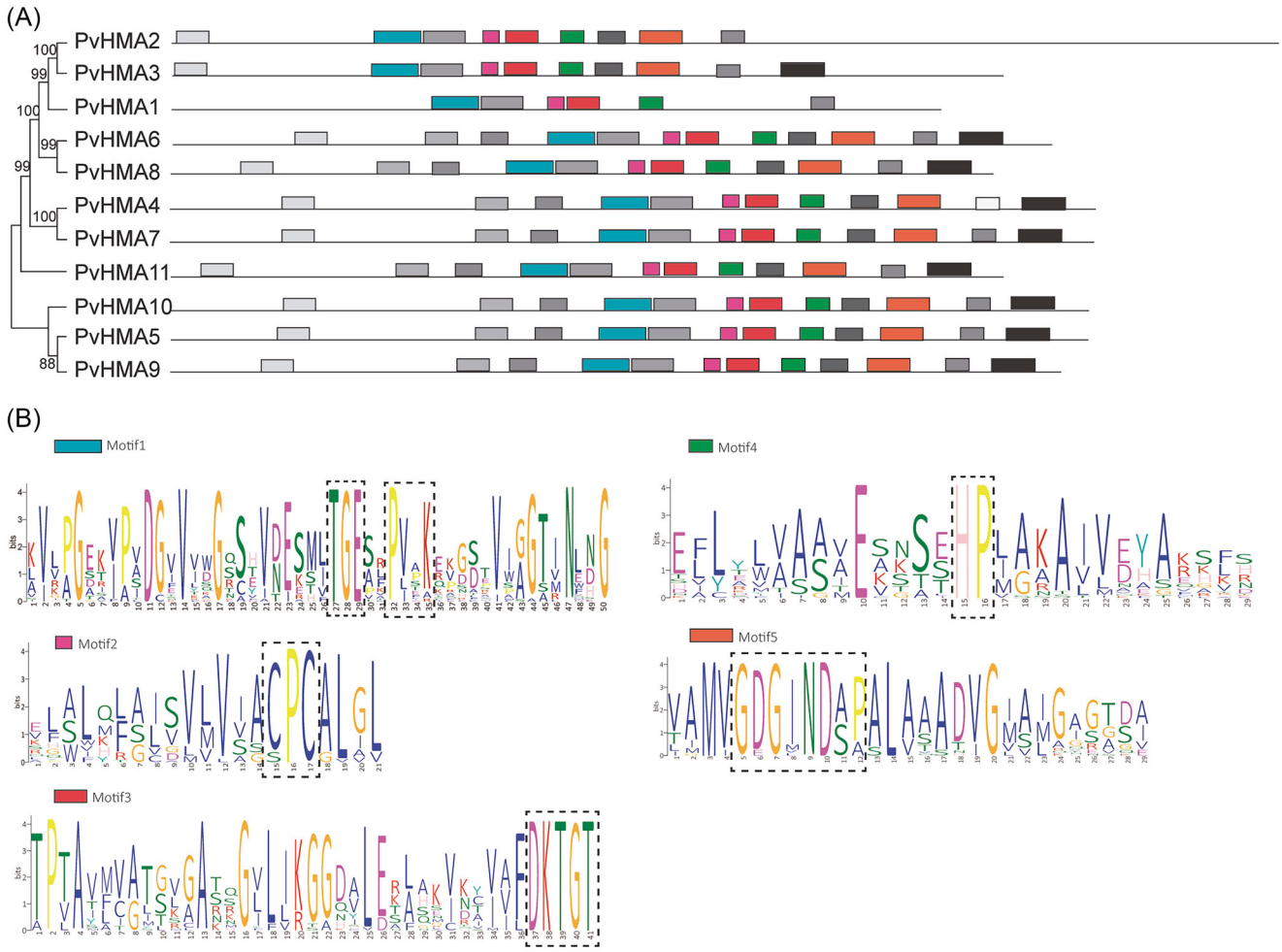

FIGURE 1 Structural characteristics of the heavy metal ATPase (HMA) family in *Phaseolus vulgaris*. (A) The left panel shows a phylogenetic tree constructed from aligned protein sequences using the maximum likelihood method. Bootstrap support values (10,000 replicates) are indicated at internal nodes. The right panel displays conserved motifs identified by the MEME tool, with each colored rectangle representing a distinct motif. Protein sequences are organized according to their phylogenetic groups. (B) Dashed lines highlight motifs that contain conserved sequences characteristic of the HMA family.

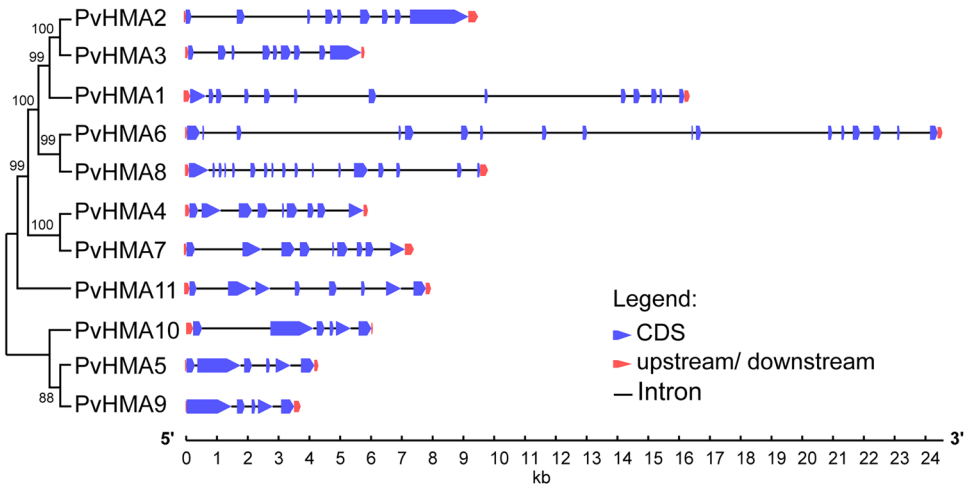

FIGURE 2 Schematic structure of *PvHMA* genes in *Phaseolus vulgaris*. Schematic representation of the exon–intron organization. Black lines indicate introns, blue arrows denote exons, and red arrows represent the 5′ and 3′ untranslated regions (UTRs). The phylogenetic tree was constructed using the maximum likelihood method, with bootstrap support values (10,000 replicates) shown at internal nodes.

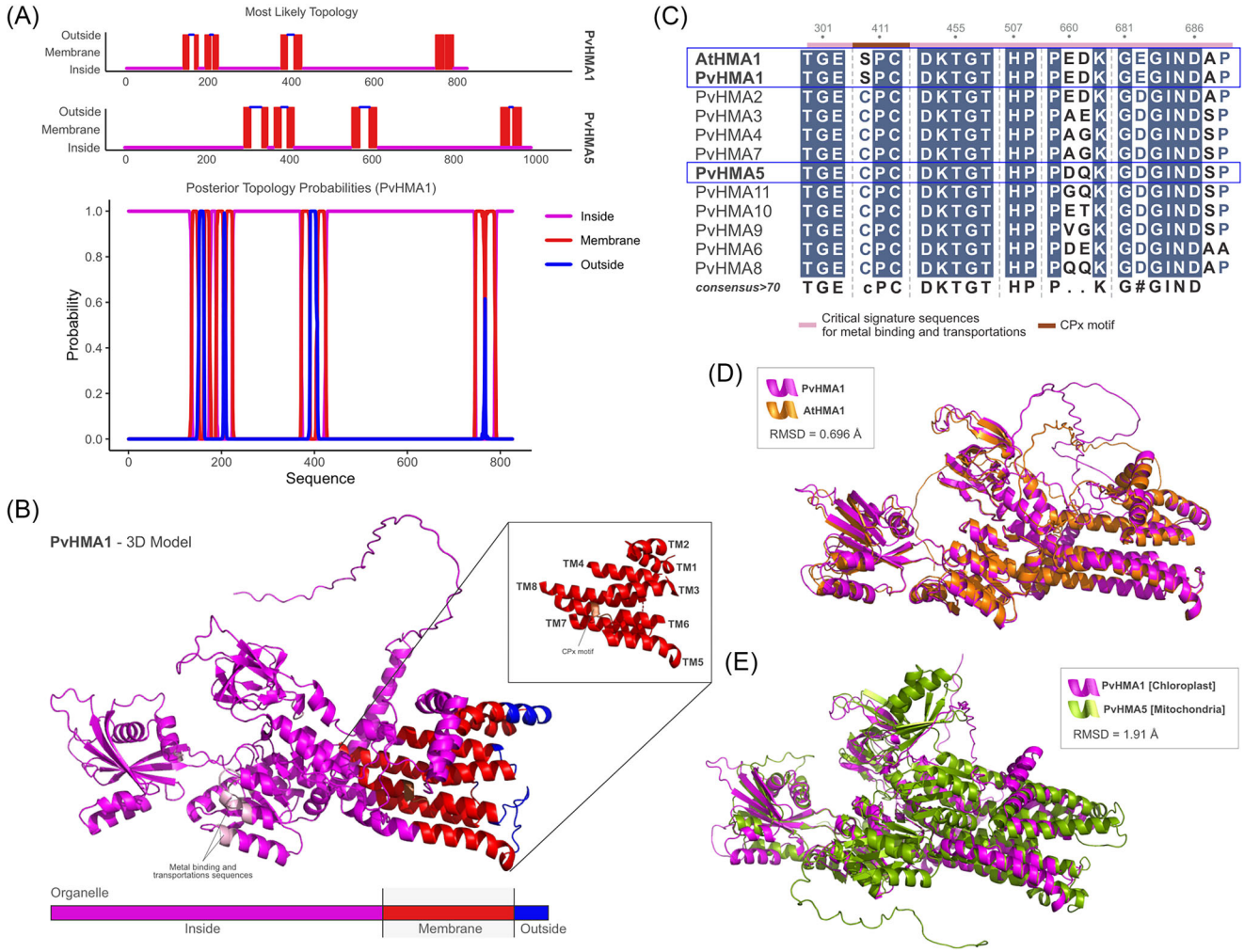

FIGURE 3 Three-dimensional (3D) modeling and structural analysis of PvHMA proteins. (A) Predicted topology of PvHMA1 and PvHMA5, with a probability graph illustrating the transmembrane regions of the PvHMA1 sequence. (B) 3D structure of PvHMA1 based on DeepTMHMM predictions, highlighting eight transmembrane domains and the CPx motif (indicated by a square). (C) Sequence alignment of *Arabidopsis thaliana* HMA1 (AtHMA1) with all PvHMA proteins, emphasizing metal-binding sites and conserved motifs. The blue rectangle marks PvHMA1/AtHMA1 and PvHMA5, which localize to different organelles. (D–E) Structural comparison of 3D models: (D) PvHMA1 versus AtHMA1, and (E) PvHMA1 (chloroplast-localized) versus PvHMA5 (mitochondria-localized). Structural similarity is indicated by root-mean-square deviation (RMSD) (Å) values. HMA, heavy metal ATPase.

3.3 | Comparative phylogenetic analysis of *HMA* genes in common bean, rice, soybean, and *A. thaliana*

To investigate the evolutionary relationships among HMA transporters across plant species, a phylogenetic tree was constructed using the full-length protein sequences of 11 *P. vulgaris* HMAs (PvHMA1–11), 20 soybean HMAs (GmHMA1–20), eight *A. thaliana* HMAs (AtHMA1–8), and nine rice HMAs (OsHMA1–9). The resulting phylogenetic tree revealed the formation of six major subfamilies, consistent with previous classifications (Fang et al., 2016; Williams & Mills, 2005) (Figure 4). Subfamilies I and II are associated with the transport of Zn, Cd, Pb, and Co. These groups included PvHMA1, -2, and -3, as well as AtHMA1–4 from *A. thaliana*, OsHMA1–3 from *O. sativa*, and five soybean homologs (GmHMA5, -13, -14, -18, and -19). The subfamily I contained PvHMA1, AtHMA1, and two soybean sequences (GmHMA5 and 19), suggesting a conserved functional group. The subfamily II positioned PvHMA2 close to AtHMA2, -3, and -4, while PvHMA3 clustered with GmHMA12 (Figure 4). The subfamilies III through VI are primarily associated with Cu transport and potentially Ag, as previously reported (Williams & Mills, 2005). This broader group included PvHMA4, -5, -6, -7, -8, -9, -10, and -11, as well as AtHMA5–8, OsHMA4–9, and 15 soybean HMA genes (Figure 4). Within subfamily III, PvHMA5, -10, and -11 grouped closely with AtHMA5, while PvHMA9 clustered with OsHMA4 and GmHMA3 and -17. Subfamily IV included PvHMA4 and PvHMA7 alongside AtHMA7 and

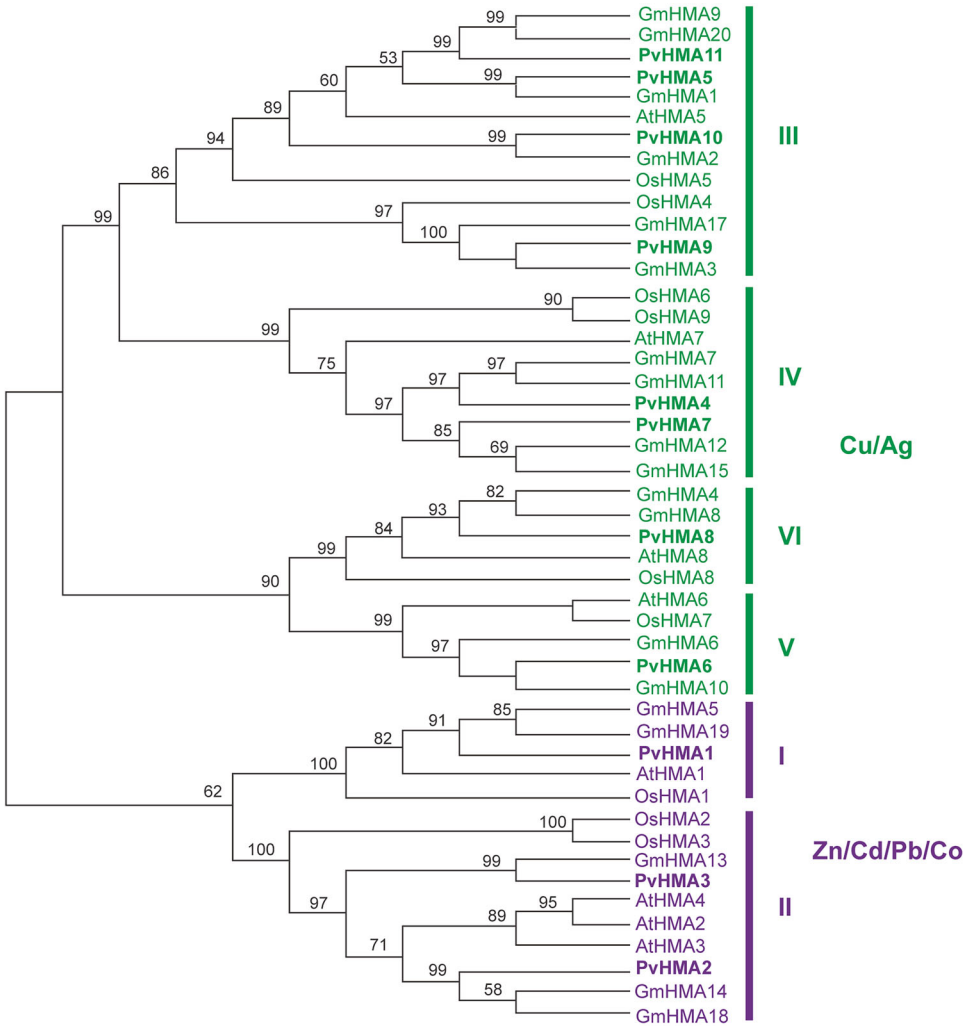

FIGURE 4 Phylogenetic relationships among heavy metal ATPase (HMA) protein sequences. An unrooted phylogenetic tree was constructed using the maximum likelihood method based on predicted HMA protein sequences. Bootstrap values (10,000 replicates) are shown at internal nodes. Sequences are color-coded by the functional group: green for the Cu/Ag clade and purple for the Zn/Cd/Pb/Co clade. *Phaseolus vulgaris* HMA sequences (PvHMA1 to PvHMA11) are highlighted in bold. The soybean genes are identified as GmHMA1–20, *Arabidopsis thaliana* sequences as AtHMA1–7, and rice sequences as OsHMA1–9. Corresponding ID information is provided in Supporting Information S1.

OsHMA6 and -9. Subfamilies V and VI were more distinct, with PvHMA6 closely related to AtHMA6, and PvHMA8 aligning with AtHMA8 and OsHMA8 (Figure 4). These phylogenetic relationships suggest functional conservation and diversification of HMA genes across dicot and monocot lineages, with PvHMA members represented in all six subfamilies, indicating a broad evolutionary distribution and potential functional specialization.

3.4 | Tissue-specific expression patterns and cis-regulatory element analysis of PvHMA genes

To gain further insights into the potential molecular roles of *PvHMA* genes, we examined their in silico expression profiles across various tissues using transcriptome data available. Among all genes analyzed, *PvHMA9* and *PvHMA10* exhibited the lowest transcriptional activity across tissues (Figure 5). In contrast, *PvHMA3* and *PvHMA4* showed preferential expression in mature pods and roots, while *PvHMA8* displayed a predominantly leaf-specific expression pattern. *PvHMA2* and *PvHMA5* were more highly expressed in stems, fruits, and roots. Broad expression across all tissues was observed for *PvHMA1*, *PvHMA6*, *PvHMA7*, *PvHMA8*, and *PvHMA11*, with particularly high transcript levels for *PvHMA1*, *PvHMA7*, and *PvHMA8*, and moderate expression for *PvHMA6* and *PvHMA11* (Figure 5).

To support the expression data, we performed a promoter analysis of the 1000 bp upstream regions of the *PvHMA* genes, identifying putative cis-regulatory elements using the PlantCARE database. For interpretative clarity,

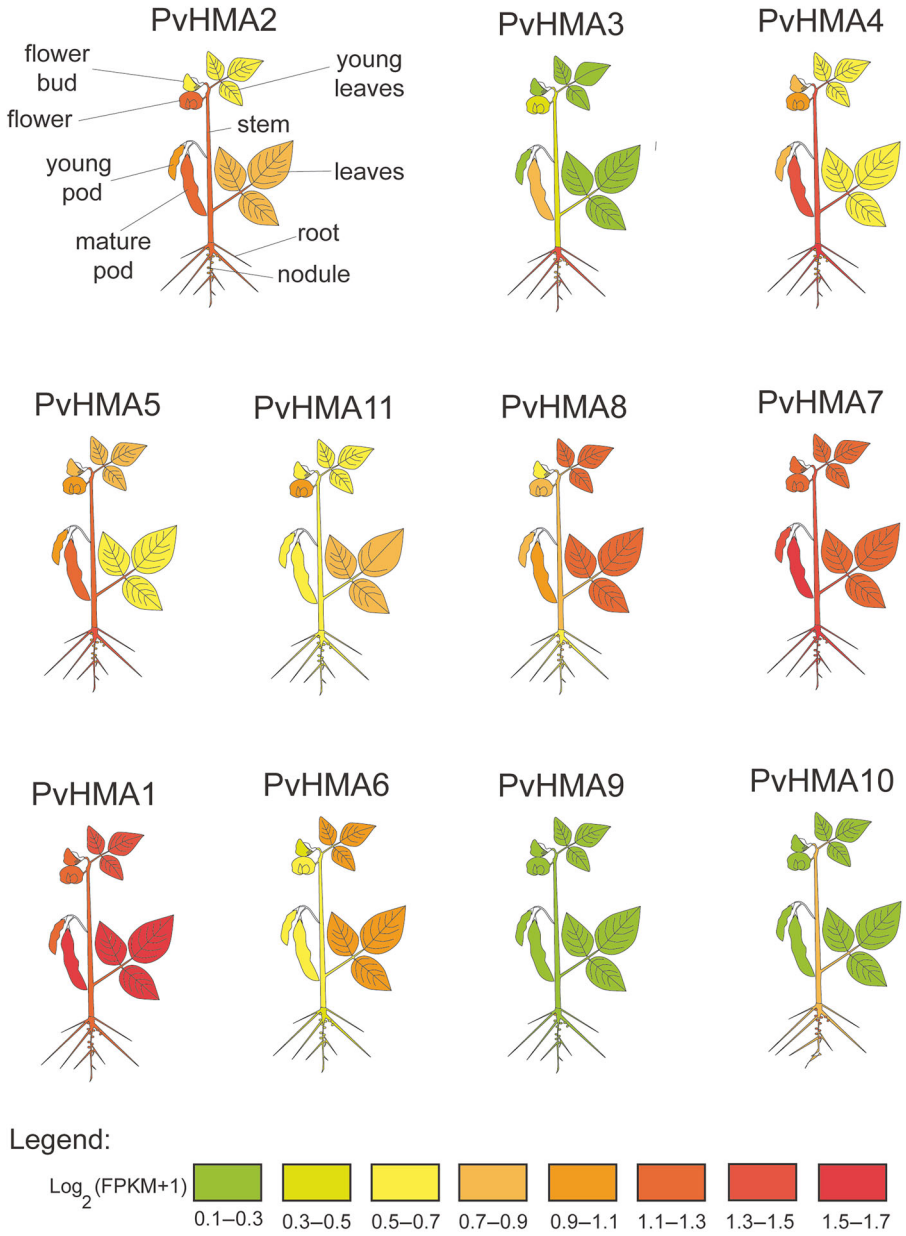

FIGURE 5 Organ-specific expression patterns of *PvHMA* gene during development. RNA-seq data from the Phytozome database (www.phytozome.net) were mapped to *PvHMA* genes to assess their expression across nine organs: flower bud, mature flower, young pod, mature pod, young leaves, mature leaves, stem, root, and nodules. Expression levels are visualized as a heatmap, with color intensity representing $\log_2$ fragments per kilobase million (FPKM) values—ranging from green (low expression) to red (high expression). HMA, heavy metal ATPase.

the elements were categorized into five functional groups: (i) DNA/protein-binding, (ii) biotic/abiotic stress-responsive, (iii) light-responsive, (iv) hormone/metabolism-related, and (v) others. Consistent with their low expression, *PvHMA9* and *PvHMA10* contained the fewest regulatory elements (five and six, respectively) (Supporting Information S7). Notably, *PvHMA3*, which is root-specific, lacked light-responsive elements, while *PvHMA8*, which is highly expressed in leaves, contained the highest number of light-associated elements, suggesting light-dependent transcriptional regulation. Promoters of *PvHMA7*, *PvHMA8*, and *PvHMA11* contained elements from all five functional categories, supporting their broad expression and potential involvement in diverse physiological processes. Due to the location of *PvHMA6* at the 5′ end of scaffold_403, promoter sequence data could not be retrieved, preventing regulatory analysis for this gene.

In summary, *PvHMA1*, *PvHMA2*, *PvHMA5*, *PvHMA6*, *PvHMA7*, and *PvHMA11* exhibit broad expression across multiple tissues, indicating roles in general HM homeostasis. In contrast, *PvHMA3*, *PvHMA4*, *PvHMA8*, and *PvHMA10* show more restricted, tissue-specific expression patterns, pointing to specialized functions in metal transport and reg-

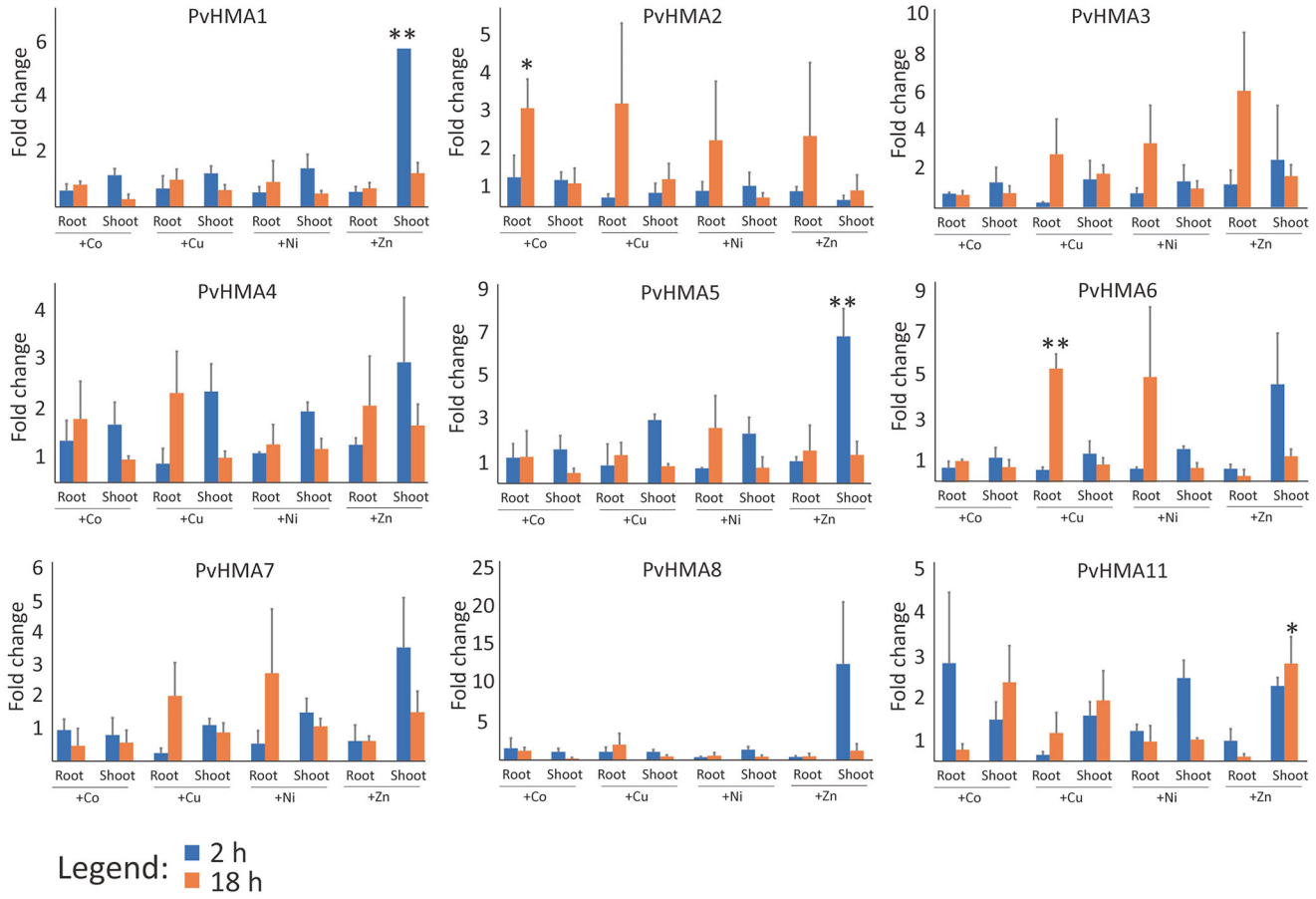

FIGURE 6 Expression of *PvHMA* genes in response to heavy metal exposure. Transcript levels of *PvHMA* genes were measured by quantitative real-time PCR (RT-qPCR) in roots and aerial parts of plants treated with Co (50 μM), Cu (100 μM), Ni (150 μM), or Zn (200 μM) for 2 h (blue bars) and 18 h (orange bars). Expression values were normalized to a constitutive reference gene, and results represent the mean of two to three biological replicates (see Section 2), each with three technical repetitions. At least two plants were used per biological replicate. Error bars indicate standard error of the mean. Statistical significance was determined using a *t*-test: $*p < 0.1$; $**p < 0.05$. HMA, heavy metal ATPase.

ulation. These expression trends closely align with the type and abundance of cis-regulatory elements identified in their promoters.

3.5 | Expression profiles of PvHMA genes in response to heavy metal stresses

To assess both early-transient and delayed gene inductions, the transcriptional response of PvHMA genes to HM exposure was measured at 2 and 18 h after treatment. The RT-qPCR was performed on root and shoot tissues following treatments with Zn^{2+}, Cu^{2+}, Co^{2+}, and Ni^{2+}. Of the 11 *PvHMA* genes analyzed, nine were expressed under at least one metal treatment, while *PvHMA9* and *PvHMA10* showed no detectable expression across all conditions (Figure 6). Significant transcriptional induction of *PvHMA1* and *PvHMA5* was observed in shoots after 2 h of Zn^{2+} exposure, with expression levels markedly higher than untreated controls; however, this induction diminished by 18 h. Conversely, *PvHMA11* exhibited a progressive and sustained increase in expression throughout zinc treatment, indicating a delayed yet persistent response (Figure 6). Under Co^{2+} treatment, *PvHMA2* was specifically upregulated in roots, suggesting involvement in cobalt transport or detoxification mechanisms. Cu^{2+} exposure elicited elevated expression of *PvHMA6*, predominantly in shoots. Notably, none of the *PvHMA* genes responded transcriptionally to Ni^{2+} under the tested conditions. These results demonstrate that *PvHMA* genes are differentially expressed depending on the specific HM and tissue type, indicating that individual transporters have specialized roles, contributing to metal-specific homeostasis and detoxification mechanisms in *P. vulgaris*.

4 | DISCUSSION

The common bean plays a pivotal role in global food security, serving as a major dietary protein and micronutrient source, especially in low- and middle-income countries. Effi-

cient metal homeostasis is essential for its productivity and nutritional value. HMAs are integral membrane transporters involved in the uptake, transport, sequestration, and detoxification of essential and nonessential metals in plants. While these proteins have been characterized in several model and crop species (Fang et al., 2016; Zhiguo et al., 2018), their diversity and function in *P. vulgaris* remained largely unexplored. Broad phylogenetic comparisons revealed that *P. vulgaris HMA* genes group into six distinct clades, consistent with the established *HMA* subfamily classification in other angiosperms (Baxter et al., 2003; Tehseen et al., 2010). The high conservation of domain structure and motif composition across these groups supports the notion that the ancestral angiosperm genome contained at least six core *HMA* genes (Axelsen & Palmgren, 2001; Hanikenne & Baurain, 2014).

The HMA1 transporter has been shown to respond to Zn stress in both *A. thaliana* and rice (Kim et al., 2009). Localized at the chloroplast envelope, it protects the organelle from Zn overaccumulation by translocating the metal to the cytoplasm (Kim et al., 2009). HMA1 plays a crucial role in the protective function of Cu/Zn SOD enzyme in above-ground tissues by providing essential metal cofactors for Cu/Zn SOD activity (Boutigny et al., 2014; Kim et al., 2009). Consistent with previous findings, the common bean homolog of HMA1 contained a chloroplast-targeting peptide signal (Supporting Information S4). Its function in Zn homeostasis in chlorophyllous tissues is supported by its differential expression upon Zn stress in shoots and reproductive organs (Figures 5 and 6) and by the presence of light-responsive cis-elements in its promoter region (Supporting Information S7). While HMA1 has been shown to transport Cu in *A. thaliana* actively (Seigneurin-Berny et al., 2006), our analysis did not reveal an expression response to excessive Cu stress in *PvHMA1* (Figure 6). Despite this, PvHMA1 shares similarities with AtHMA1 regarding subcellular localization (Supporting Information S4), protein structure (Figure 3D), and Zn transport (Figure 6). However, their roles in Cu homeostasis may differ. We observed a basal expression of *PvHMA1* in roots that were not differentially expressed by metal exposure (Figure 6). Similar findings have been reported in other plants (D. Li et al., 2015; Seigneurin-Berny et al., 2006), suggesting a parallel function of HMA1 in non-green plastids.

In *A. thaliana*, the HMA2 and HMA4 exhibit redundant functions, sharing similar expression patterns upon Cd and Zn overexposure and predominantly localizing in cells surrounding root vascular vessels (Eren & Argüello, 2004; Hussain et al., 2004). Both transporters facilitate the translocation of Zn from root pericycle cells into the vascular system for delivery to above-ground organs (Hanikenne & Bouché, 2023). Our phylogenetic analysis revealed that a single gene represents the closest homologs of *AtHMA2* and *AtHMA4* in the common bean, *PvHMA2* (Figure 4). Like AtHMA2/4, PvHMA2 is associated with the secretory pathway (Supporting Information S4), translocating metals from the cytoplasm to the extracellular environment. *PvHMA2* exhibited strong expression in vascular tissues and roots (Figure 5) with an overall tendency to be upregulated upon metal treatments (Figure 6). In *A. thaliana*, high levels of *AtHMA2* mRNA were detected in plants treated with various metals, including Ag, Co, Cu, Cd, Mn, and Ni. However, only Zn and Cd were shown to increase the metal-dependent phosphorylation and ATPase activity of HMA2 (Eren & Argüello, 2004). Interestingly, in common beans, *PvHMA2* expression was detected by 40 nm ZnO nanoparticle treatment (da Cruz et al., 2019). These findings suggest that PvHMA2 plays a role in Zn homeostasis similar to AtHMA2/4, although further studies are needed to clarify how different metal species influence its ATPase activity and transport function. Altogether, our phylogenetic and transcriptional data support the hypothesis that PvHMA2 shares conserved biological functions with its Arabidopsis homologs.

Cu is an essential micronutrient for numerous physiological processes in plants, with roots serving as the primary site for its uptake. Inadequate Cu availability disrupts normal root and leaf development, reduces chlorophyll synthesis, and impairs photosynthetic performance (Hong et al., 2015). Our results indicate that *PvHMA6* plays a role in Cu homeostasis in *P. vulgaris*. This gene displayed strong expression in root tissues and moderate expression in photosynthetic organs (Figure 5), and its transcription was significantly induced following Cu exposure (Figure 6). These patterns suggest a functional role in both Cu uptake from the soil and internal redistribution. In support of this, PvHMA6 similar to its closest homologs in *A. thaliana* (AtHMA8) (Figure 4) and *M. truncatula* (MtHMA4) (Ma et al., 2021) are chloroplast-localized transporters (Supporting Information S4). In addition, AtHMA8 and MtHMA4 are reported to respond to Cu stress (Ma et al., 2021; Sautron et al., 2016). AtHMA8, in particular, has been shown to supply Cu to chloroplastic enzymes such as Cu/Zn SOD and plastocyanin, which are crucial for oxidative stress defense and the electron transport chain during photosynthesis (Abdel-Ghany et al., 2005). Taken together, these findings support a dual role for PvHMA6 in facilitating Cu acquisition at the root level and in supplying Cu to chloroplasts to sustain photosynthetic function.

Our investigation indicates that *PvHMA5* and *PvHMA11* are involved in Zn homeostasis in common beans. Both genes responded to HM exposure, with *PvHMA5* showing rapid increase in transcript expression within 2 hours, while *PvHMA11* displayed a delayed response, becoming evident after 18 h (Figure 6). Based on their high sequence similarity to GmHMA1/9 in soybean and predicted localization signals, PvHMA5 and PvHMA11 are likely targeted to the mitochondrial membrane (Fang et al., 2016; Supporting Information S4). These homologous transporters in soybean are

known to respond to Cd, prompting investigation into whether PvHMA5 and PvHMA11 share this sensitivity. Interestingly, under our experimental conditions, neither gene responded to Cd, suggesting that these transporters may have diverged functionally in *P. vulgaris*. Unlike their closest homolog in *A. thaliana*, AtHMA5—a plasma membrane Cu transporter that is not responsive to Cd, Zn, or Fe (Andrés-Colás et al., 2006)—*PvHMA5* and *PvHMA11* appear to be specifically responsive to Zn. These findings suggest that PvHMA5 and PvHMA11 have evolved distinct roles in Zn regulation in common beans, differing from their counterparts in both soybean and *A. thaliana*.

5 | CONCLUSION

Our findings offered a comprehensive perspective on the *HMA* gene family in common beans. The 11 transporters observed in this study were categorized into six distinct clusters, each exhibiting a consistent gene structure and distribution of motifs. The expression studies provide initial insights into the role of HMA in the absorption, storage, and transit of metals in the roots, stems, and leaves of the common bean. Our findings will help to understand the biological function of the individuals involved in metal balance during the growth of *P. vulgaris*.

AUTHOR CONTRIBUTIONS

Wenderson Felipe Costa Rodrigues: Data curation; formal analysis; investigation; methodology; validation; visualization; writing—original draft; writing—review and editing. **Laura Oliveira Pires**: Data curation; formal analysis; investigation; methodology; validation; visualization; writing—original draft; writing—review and editing. **Lucas Roberto Oliveira**: Data curation; formal analysis; investigation; methodology; writing—original draft. **Juliane K. Ishida**: Conceptualization; data curation; formal analysis; funding acquisition; methodology; project administration; resources; supervision; validation; visualization; writing—original draft; writing—review and editing.

ACKNOWLEDGMENTS

This study was funded by the Serrapilheira Institute (R-2111-40087), the Research Support Foundation of the State of Minas Gerais (FAPEMIG) (APQ-02786-21), and the Science Without Borders Program from the Brazilian Federal Government (88887.092433/2015-00). Additionally, this study received partial funding from the Coordenação de Aperfeiçoamento de Pessoal de Nível Superior–Brazil (CAPES), Finance Code 001.

The Article Processing Charge for the publication of this research was funded by the Coordenação de Aperfeiçoamento de Pessoal de Nível Superior - Brasil (CAPES) (ROR identifier: 00x0ma614).

CONFLICT OF INTEREST STATEMENT

The authors declare no conflicts of interest.

ORCID

Juliane K. Ishida https://orcid.org/0000-0002-0956-7578

REFERENCES

Abd-Alla, M. H., Al-Amri, S. M., & El-Enany, A.-W. E. (2023). Enhancing rhizobium–legume symbiosis and reducing nitrogen fertilizer use are potential options for mitigating climate change. *Agriculture*, *13*(11), 2092. https://doi.org/10.3390/agriculture13112092

Abdel-Ghany, S. E., Müller-Moulé, P., Niyogi, K. K., Pilon, M., & Shikanai, T. (2005). Two P-type ATPases are required for copper delivery in *Arabidopsis thaliana* chloroplasts. *The Plant Cell*, *17*, 1233–1251. https://doi.org/10.1105/tpc.104.030452

Alloway, B. J. (2013). Heavy metals and metalloids as micronutrients for plants and animals. In B. J. Alloway (Ed.), *Heavy metals in soils: Trace metals and metalloids in soils and their bioavailability* (pp. 195–209). Springer.

Andrés-Colás, N., Sancenón, V., Rodríguez-Navarro, S., Mayo, S., Thiele, D. J., Ecker, J. R., Puig, S., & Peñarrubia, L. (2006). The Arabidopsis heavy metal P-type ATPase HMA5 interacts with metallochaperones and functions in copper detoxification of roots. *The Plant Journal*, *45*, 225–236. https://doi.org/10.1111/j.1365-313X.2005.02601.x

Argüello, J. M., Eren, E., & González-Guerrero, M. (2007). The structure and function of heavy metal transport P_{1B}-ATPases. *Biometals*, *20*, 233–248. https://doi.org/10.1007/s10534-006-9055-6

Atafar, Z., Mesdaghinia, A., Nouri, J., Homaee, M., Yunesian, M., Ahmadimoghaddam, M., & Mahvi, A. H. (2010). Effect of fertilizer application on soil heavy metal concentration. *Environmental Monitoring and Assessment*, *160*, 83–89. https://doi.org/10.1007/s10661-008-0659-x

Axelsen, K. B., & Palmgren, M. G. (2001). Inventory of the superfamily of P-type ion pumps in Arabidopsis. *Plant Physiology*, *126*, 696–706. https://doi.org/10.1104/pp.126.2.696

Bailey, T. L., Boden, M., Buske, F. A., Frith, M., Grant, C. E., Clementi, L., Ren, J., Li, W. W., & Noble, W. S. (2009). MEME SUITE: Tools for motif discovery and searching. *Nucleic Acids Research*, *37*, W202–W208. https://doi.org/10.1093/nar/gkp335

Batool, T. S., Aslam, R., Gul, A., Paracha, R. Z., Ilyas, M., De Abreu, K., Munir, F., Amir, R., & Williams, L. E. (2023). Genome-wide analysis of heavy metal ATPases (*HMAs*) in Poaceae species and their potential role against copper stress in *Triticum aestivum*. *Scientific Reports*, *13*, 7551. https://doi.org/10.1038/s41598-023-32023-7

Baxter, I., Tchieu, J., Sussman, M. R., Boutry, M., Palmgren, M. G., Gribskov, M., Harper, J. F., & Axelsen, K. B. (2003). Genomic comparison of P-type ATPase ion pumps in Arabidopsis and rice. *Plant Physiology*, *132*, 618–628. https://doi.org/10.1104/pp.103.021923

Bjellqvist, B., Hughes, G. J., Pasquali, C., Paquet, N., Ravier, F., Sanchez, J.-C., Frutiger, S., & Hochstrasser, D. (1993). The focusing positions of polypeptides in immobilized pH gradients can be predicted from their amino acid sequences. *Electrophoresis*, *14*, 1023–1031. https://doi.org/10.1002/elps.11501401163

Boutigny, S., Sautron, E., Finazzi, G., Rivasseau, C., Frelet-Barrand, A., Pilon, M., Rolland, N., & Seigneurin-Berny, D. (2014). HMA1 and PAA1, two chloroplast-envelope P_{1B}-ATPases, play distinct roles in chloroplast copper homeostasis. *Journal of Experimental Botany*, *65*, 1529–1540. https://doi.org/10.1093/jxb/eru020

Da Cruz, T. N. M., Savassa, S. M., Montanha, G. S., Ishida, J. K., De Almeida, E., Tsai, S. M., Lavres Junior, J., & Pereira De Carvalho, H. W. (2019). A new glance on root-to-shoot in vivo zinc transport and time-dependent physiological effects of $ZnSO_4$ and ZnO nanoparticles on plants. *Scientific Reports*, *9*, Article 10416. https://doi.org/10.1038/s41598-019-46796-3

Eastman, P., Swails, J., Chodera, J. D., McGibbon, R. T., Zhao, Y., Beauchamp, K. A., Wang, L. P., Simmonett, A. C., Harrigan, M. P., Stern, C. D., Wiewiora, R. P., Brooks, B. R., & Pande, V. S. (2017). OpenMM 7: Rapid development of high performance algorithms for molecular dynamics. *PLoS Computational Biology*, *13*, e1005659. https://doi.org/10.1371/journal.pcbi.1005659

Emanuelsson, O., Brunak, S., von Heijne, G., & Nielsen, H. (2007). Locating proteins in the cell using TargetP, SignalP and related tools. *Nature Protocols*, *2*, 953–971. https://doi.org/10.1038/nprot.2007.131

Eren, E., & ArgüEllo, J. M. (2004). Arabidopsis HMA2, a divalent heavy metal-transporting P_{1B}-type ATPase, is involved in cytoplasmic Zn^{2+} homeostasis. *Plant Physiology*, *136*, 3712–3723. https://doi.org/10.1104/pp.104.046292

Fang, X., Wang, L., Deng, X., Wang, P., Ma, Q., Nian, H., Wang, Y., & Yang, C. (2016). Genome-wide characterization of soybean *P_{1B}-ATPases* gene family provides functional implications in cadmium responses. *BMC Genomics*, *17*, Article 376. https://doi.org/10.1186/s12864-016-2730-2

Farley, R. A. (2012). Active ion transport by ATP-driven ion pumps. In N. Sperelakis (Ed.), *Cell physiology source book* (pp. 167–177). Academic Press.

Hallgren, J., Tsirigos, K. D., Damgaard Pedersen, M., Juan, J., Armenteros, A., Marcatili, P., Nielsen, H., Krogh, A., & Winther, O. (2022). DeepTMHMM predicts alpha and beta transmembrane proteins using deep neural networks. *BioRxiv*. https://doi.org/10.1101/2022.04.08.487609

Hanikenne, M., & Baurain, D. (2014). Origin and evolution of metal P-type ATPases in Plantae (Archaeplastida). *Frontiers in Plant Science*, *4*, Article 544. https://doi.org/10.3389/fpls.2013.00544

Hanikenne, M., & Bouché, F. (2023). Iron and zinc homeostasis in plants: A matter of trade-offs. *Journal of Experimental Botany*, *74*(18), 5426–5430. https://doi.org/10.1093/jxb/erad304

Hawkes, S. J. (1997). What is a heavy metal? *Journal of Chemical Education*, *74*, 1374. https://doi.org/10.1021/ed074p1374

Hirayama, T., Kieber, J. J., Hirayama, N., Kogan, M., Guzman, P., Nourizadeh, S., Alonso, J. M., Dailey, W. P., Dancis, A., & Ecker, J. R. (1999). RESPONSIVE-TO-ANTAGONIST1, a Menkes/Wilson disease–related copper transporter, is required for ethylene signaling in *Arabidopsis*. *Cell*, *97*, 383–393. https://doi.org/10.1016/S0092-8674(00)80747-3

Hong, J., Rico, C. M., Zhao, L. J., Adeleye, A. S., Keller, A. A., Peralta-Videa, J. R., & Gardea-Torresdey, J. L. (2015). Toxic effects of copper-based nanoparticles or compounds to lettuce (*Lactuca sativa*) and alfalfa (*Medicago sativa*). *Environmental Science. Processes & Impacts*, *17*, 177–185.

Hu, B., Jin, J., Guo, A.-Y., Zhang, H., Luo, J., & Gao, G. (2015). GSDS 2.0: An upgraded gene feature visualization server. *Bioinformatics*, *31*, 1296–1297.

Hussain, D., Haydon, M. J., Wang, Y., Wong, E., Sherson, S. M., Young, J., Camakaris, J., Harper, J. F., & Cobbett, C. S. (2004). P-type ATPase heavy metal transporters with roles in essential zinc homeostasis in Arabidopsis. *The Plant cell*, *16*, 1327–1339. https://doi.org/10.1105/tpc.020487

Jumper, J., Evans, R., Pritzel, A., Green, T., Figurnov, M., Ronneberger, O., Tunyasuvunakool, K., Bates, R., Žídek, A., Potapenko, A., Bridgland, A., Meyer, C., Kohl, S. A. A., Ballard, A. J., Cowie, A., Romera-Paredes, B., Nikolov, S., Jain, R., Adler, J., … Hassabis, D. (2021). Highly accurate protein structure prediction with AlphaFold. *Nature*, *596*, 583–589. https://doi.org/10.1038/s41586-021-03819-2

Katoh, K., & Standley, D. M. (2013). MAFFT multiple sequence alignment software version 7: Improvements in performance and usability. *Molecular Biology and Evolution*, *30*(4), 772–780. https://doi.org/10.1093/molbev/mst010

Kim, Y.-Y., Choi, H., Segami, S., Cho, H.-T., Martinoia, E., Maeshima, M., & Lee, Y. (2009). AtHMA1 contributes to the detoxification of excess Zn(II) in Arabidopsis. *The Plant Journal*, *58*, 737–753. https://doi.org/10.1111/j.1365-313X.2009.03818.x

Kühlbrandt, W. (2004). Biology, structure and mechanism of P-type ATPases. *Nature Reviews Molecular Cell Biology*, *5*, 282–295. https://doi.org/10.1038/nrm1354

Kumar, S., Stecher, G., & Tamura, K. (2016). MEGA7: Molecular evolutionary genetics analysis version 7.0 for bigger datasets. *Molecular Biology and Evolution*, *33*, 1870–1874. https://doi.org/10.1093/molbev/msw054

Lee, S., Kim, Y.-Y., Lee, Y., & An, G. (2007). Rice P_{1B}-type heavy-metal ATPase, OsHMA9, is a metal efflux protein. *Plant Physiology*, *145*, 831–842. https://doi.org/10.1104/pp.107.102236

Lescot, M., Déhais, P., Thijs, G., Marchal, K., Moreau, Y., Van de Peer, Y., Rouzé, P., & Rombauts, S. (2002). PlantCARE, a database of plant cis-acting regulatory elements and a portal to tools for in silico analysis of promoter sequences. *Nucleic Acids Research*, *30*, 325–327. https://doi.org/10.1093/nar/30.1.325

Letunic, I., Khedkar, S., & Bork, P. (2021). SMART: Recent updates, new developments and status in 2020. *Nucleic Acids Research*, *49*(D1), D458–D460. https://doi.org/10.1093/nar/gkaa937

Li, D., Xu, X., Hu, X., Liu, Q., Wang, Z., Zhang, H., Wang, H., Wei, M., Wang, H., Liu, H., & Li, C. (2015). Genome-wide analysis and heavy metal-induced expression profiling of the HMA gene family in *Populus trichocarpa*. *Frontiers in Plant Science*, *6*, Article 1149. https://doi.org/10.3389/fpls.2015.01149

Li, N., Xiao, H., Sun, J., Wang, S., Wang, J., Chang, P., Zhou, X., Lei, B., Lu, K., Luo, F., Shi, X., & Li, J. (2018). Genome-wide analysis and expression profiling of the *HMA* gene family in *Brassica napus* under cd stress. *Plant and Soil*, *426*, 365–381. https://doi.org/10.1007/s11104-018-3637-2

Ma, Y., Wei, N., Wang, Q., Liu, Z., & Liu, W. (2021). Genome-wide identification and characterization of the heavy metal ATPase (HMA) gene family in *Medicago truncatula* under copper stress. *International Journal of Biological Macromolecules*, *193*, 893–902. https://doi.org/10.1016/j.ijbiomac.2021.10.197

Mirdita, M., Schütze, K., Moriwaki, Y., Heo, L., Ovchinnikov, S., & Steinegger, M. (2022). ColabFold: Making protein folding accessible to all. *Nature Methods*, *19*(6), 679–682. https://doi.org/10.1038/s41592-022-01488-1

Morel, M., Crouzet, J., Gravot, A., Auroy, P., Leonhardt, N., Vavasseur, A., & Richaud, P. (2009). AtHMA3, a P_{1B}-ATPase allowing Cd/Zn/Co/Pb vacuolar storage in Arabidopsis. *Plant physiology*, *149*, 894–904. https://doi.org/10.1104/pp.108.130294

Moreno, I., Norambuena, L., Maturana, D., Toro, M., Vergara, C., Orellana, A., Zurita-Silva, A., & Ordenes, V. R. (2008). $AtHMA_1$

is a thapsigargin-sensitive Ca^{2+}/heavy metal pump. *The Journal of Biological Chemistry*, *283*, 9633–9641. https://doi.org/10.1074/jbc.M800736200

Mortvedt, J. J. (1996). Heavy metal contaminants in inorganic and organic fertilizers. *Fertilizer Research*, *43*, 55–61. https://doi.org/10.1007/BF00747683

Murube, E., Beleggia, R., Pacetti, D., Nartea, A., Frascarelli, G., Lanzavecchia, G., Bellucci, E., Nanni, L., Gioia, T., Marciello, U., Esposito, S., Foresi, G., Logozzo, G., Frega, G. N., Bitocchi, E., & Papa, R. (2021). Characterization of nutritional quality traits of a common bean germplasm collection. *Foods*, *10*(7), 1572. https://doi.org/10.3390/foods10071572

Navarrete, A. A., Mellis, E. V., Escalas, A., Lemos, L. N., Junior, J. L., Quaggio, J. A., Zhou, J., & Tsai, S. M. (2017). Zinc concentration affects the functional groups of microbial communities in sugarcane-cultivated soil. *Agriculture, Ecosystems & Environment*, *236*, 187–197. https://doi.org/10.1016/j.agee.2016.12.009

Nouet, C., Charlier, J.-B., Carnol, M., Bosman, B., Farnir, F., Motte, P., & Hanikenne, M. (2015). Functional analysis of the three HMA4 copies of the metal hyperaccumulator *Arabidopsis halleri*. *Journal of Experimental Botany*, *66*, 5783–5795. https://doi.org/10.1093/jxb/erv280

Palmgren, M. G., & Axelsen, K. B. (1998). Evolution of P-type ATPases. *Biochimica et Biophysica Acta*, *1365*, 37–45. https://doi.org/10.1016/S0005-2728(98)00041-3

Pedersen, P. L., & Carafoli, E. (1987). Ion motive ATPases. I. Ubiquity, properties, and significance to cell function. *Trends in Biochemical Sciences*, *12*, 146–150. https://doi.org/10.1016/0968-0004(87)90071-5

Rascio, N., & Navari-Izzo, F. (2011). Heavy metal hyperaccumulating plants: How and why do they do it? And what makes them so interesting? *Plant Science*, *180*, 169–181. https://doi.org/10.1016/j.plantsci.2010.08.016

Reich, M., Liefeld, T., Gould, J., Lerner, J., Tamayo, P., & Mesirov, J. P. (2006). GenePattern 2.0. *Nature Genetics*, *38*, 500–501. https://doi.org/10.1038/ng0506-500

Satoh-Nagasawa, N., Mori, M., Nakazawa, N., Kawamoto, T., Nagato, Y., Sakurai, K., Takahashi, H., Watanabe, A., & Akagi, H. (2012). Mutations in rice (*Oryza sativa*) heavy metal ATPase 2 (OsHMA2) restrict the translocation of zinc and cadmium. *Plant and Cell Physiology*, *53*, 213–224. https://doi.org/10.1093/pcp/pcr166

Sautron, E., Giustini, C., Dang, T., Moyet, L., Salvi, D., Crouzy, S., Rolland, N., Catty, P., & Seigneurin-Berny, D. (2016). Identification of two conserved residues involved in copper release from chloroplast PIB-1-ATPases. *Journal of Biological Chemistry*, *291*(38), 20136–20148. https://doi.org/10.1074/jbc.M115.706978

Seigneurin-Berny, D., Gravot, A., Auroy, P., Mazard, C., Kraut, A., Finazzi, G., Grunwald, D., Rappaport, F., Vavasseur, A., Joyard, J., Richaud, P., & Rolland, N. (2006). HMA1, a new Cu-ATPase of the chloroplast envelope, is essential for growth under adverse light conditions. *The Journal of biological chemistry*, *281*, 2882–2892. https://doi.org/10.1074/jbc.M508333200

Shikanai, T., Müller-Moulé, P., Munekage, Y., Niyogi, K. K., & Pilon, M. (2003). PAA1, a P-type ATPase of Arabidopsis, functions in copper transport in chloroplasts. *The Plant cell*, *15*, 1333–1346. https://doi.org/10.1105/tpc.011817

Sinclair, S. A., Sherson, S. M., Jarvis, R., Camakaris, J., & Cobbett, C. S. (2007). The use of the zinc-fluorophore, Zinpyr-1, in the study of zinc homeostasis in *Arabidopsis* roots. *New Phytologist*, *174*, 39–45. https://doi.org/10.1111/j.1469-8137.2007.02030.x

Sperotto, R. A., & Ricachenevsky, F. K. (2017). Common bean Fe biofortification using model species' lessons. *Frontiers in Plant Science*, *8*, Article 2187. https://doi.org/10.3389/fpls.2017.02187

Takahashi, R., Bashir, K., Ishimaru, Y., Nishizawa, N. K., & Nakanishi, H. (2012). The role of heavy-metal ATPases, HMAs, in zinc and cadmium transport in rice. *Plant Signaling & Behavior*, *7*, 1605–1607. https://doi.org/10.4161/psb.22454

Tehseen, M., Cairns, N., Sherson, S., & Cobbett, C. S. (2010). Metallochaperone-like genes in *Arabidopsis thaliana*. *Metallomics*, *2*, 556–564. https://doi.org/10.1039/c003484c

Teufel, F., Almagro Armenteros, J. J., Johansen, A. R., Gíslason, M. H., Pihl, S. I., Tsirigos, K. D., Winther, O., Brunak, S., von Heijne, G., & Nielsen, H. (2022). SignalP 6.0 predicts all five types of signal peptides using protein language models. *Nature Biotechnology*, *40*(7), 1023–1025. https://doi.org/10.1038/s41587-021-01156-3

Thompson, J. D., Gibson, T. J., & Higgins, D. G. (2002). *Multiple sequence alignment using ClustalW and ClustalX*. Current Protocols in Bioinformatics.

Ueno, D., Yamaji, N., Kono, I., Huang, C. F., Ando, T., Yano, M., & Ma, J. F. (2010). Gene limiting cadmium accumulation in rice. *Proceedings of the National Academy of Sciences of the United States of America*, *107*(38), 16500–16505. https://doi.org/10.1073/pnas.1005396107

Williams, L. E., & Mills, R. F. (2005). P_{1B}-ATPases—An ancient family of transition metal pumps with diverse functions in plants. *Trends in Plant Science*, *10*, 491–502. https://doi.org/10.1016/j.tplants.2005.08.008

Williams, L. E., Pittman, J. K., & Hall, J. L. (2000). Emerging mechanisms for heavy metal transport in plants. *Biochimica et Biophysica Acta (BBA)—Biomembranes*, *1465*, 104–126. https://doi.org/10.1016/S0005-2736(00)00133-4

Zhang, L., Wu, J., Tang, Z., Huang, X. Y., Wang, X., Salt, D. E., & Zhao, F. J. (2019). Variation in the *BrHMA3* coding region controls natural variation in cadmium accumulation in *Brassica rapa* vegetables. *Journal of Experimental Botany*, *70*(20), 5865–5878. https://doi.org/10.1093/jxb/erz310

Zhang, Z., Yu, Q., Du, H., Ai, W., Yao, X., Mendoza-Cózatl, D. G., & Qiu, B. (2016). Enhanced cadmium efflux and root-to-shoot translocation are conserved in the hyperaccumulator *Sedum alfredii* (Crassulaceae family). *FEBS Letters*, *590*(12), 1757–1764. https://doi.org/10.1002/1873-3468.12225

Zhiguo, E., Tingting, L., Chen, C., & Lei, W. (2018). Genome-wide survey and expression analysis of P_{1B}-ATPases in rice, maize and sorghum. *Rice Science*, *25*, 208–217. https://doi.org/10.1016/j.rsci.2018.06.004

SUPPORTING INFORMATION

Additional supporting information can be found online in the Supporting Information section at the end of this article.

How to cite this article: Rodrigues, W. F. C., Pires, L. O., Oliveira, L. R., & Ishida, J. K. (2025). Comprehensive characterization of HMA transporters in common bean: Tissue-specific expression and response to metal stress. *Crop Science*, *65*, e70188. https://doi.org/10.1002/csc2.70188